Journal of Cluster Science (2022) 33:2037–2044
https://doi.org/10.1007/s10876-021-02125-1

ORIGINAL PAPER

The Cytotoxicity Effect of Curcumin Loaded Folic Acid Conjugated-Nanoparticles on Breast Cancer Cells and Its Association with Inhibition of STAT3 Phosphorylation

Elnaz Faghfuri[1,2] · Mohsen Sagha[3] · Amir Hossein Faghfouri[4]

Received: 16 March 2021 / Accepted: 30 June 2021 / Published online: 10 July 2021

Abstract

Signal Transducer and Activator of Transcription 3 (STAT3) phosphorylation plays a key role in the transformation and proliferation of breast cancer cells. According to previous studies, STAT3 phosphorylation can be inhibited by curcumin in various cancer cells. Even so, its use is restricted due to low oral bioavailability. This study aimed to enhance curcumin solubility and bioavailability by loading it on Folic Acid-Selenium nanoparticles and determine their effect on STAT3 activation in breast cancer cell line. The synthesized nanoparticles were characterized by Fourier-transform infrared spectroscopy, Dynamic light scattering, and transmission electron microscope. MTT and western blotting methods were applied to determine the viability and protein level of MCF cell line. The size and zeta potential of nanoparticles were found to be about 130 nm and − 45 mV, respectively. The results indicated a reduction of 49.62 ± 1.85% ($p < 0.05$) in the viability and 79% ($P < 0.0001$) in the phospho-STAT3 (p-STAT3) level in the cell line tested. Curcumin-loaded folic acid conjugated nanoparticles could be an effective drug for breast cancer chemotherapy. Though, subsequent in vivo research is required to determine its efficiency and safety in clinical applications.

Keywords Nanoparticle · Curcumin · Selenium · STAT3 · MCF7

Introduction

According to the World Health Organization (WHO), breast cancer (BC) continues to be the most important cancer that kills women worldwide [1]. Many cases have been reported, and more than 450,000 women die each year from breast cancer [2]. A multidisciplinary method is employed to treat breast cancer, a combination of radiation, surgical and medical oncology.

Surgery combined with chemo-radiation is applied to treat early-stage breast cancer. Meanwhile, chemotherapy is mostly performed and has been developed as a crucial treatment for women with breast cancer [3], but these methods often non-specifically kill healthy cells and cause side effects for patients [4]. So, there is a necessity to establish new chemotherapy approaches to target cancer cells through active (receptor-mediated) or passive means. Nanoparticle (NP) mediated drug delivery has great potential to solve these problems. The developed NPs can potentially deliver therapeutic drugs to the intended site of action.

Natural compounds in dietary constituents have been shown potential as therapeutic agents against cancer, and other diseases [5]. Although their success in clinical trials has not been significant, in part owing to the low bioavailability of these compounds. Thus, to overcome this disadvantage, natural product-based nano-formulations have recently been considered. Curcumin (CUR) is a

✉ Elnaz Faghfuri
Elnaz.faghfuri@gmail.com

1 Pharmaceutical Sciences Research Center, Ardabil University of Medical Sciences, Ardabil, Iran

2 Digestive Disease Research Center, Ardabil University of Medical Sciences, Varzesh Sq., 30 Tir St., Ardabil 56136-58115, Iran

3 Research Laboratory for Embryology and Stem Cells, Department of Anatomical Sciences, School of Medicine, Ardabil University of Medical Sciences, Ardabil, Iran

4 Department of Community Nutrition, Faculty of Nutrition and Food Sciences, Tabriz University of Medical Sciences, Tabriz, Iran

lipophilic polyphenolic pigment extracted from Curcuma longa. In various studies, it has shown chemo-preventive, anti-cancer, radio, and chemo-sensitization characteristics [6]. Safety, extensive availability, low cost, and various anti-cancer roles of CUR justify its application in the treatment of cancer.

The anti-cancer ability of CUR is demonstrated by modulating several intracellular signaling pathways responsible for cell proliferation, migration, inflammation, and apoptosis [7]. It has also been shown that CUR exerts its anti-inflammatory and anti-cancer effects by targeting STAT3 signaling.

STAT3, as a signaling center where various carcinogenic signals converge, represents a potentially attractive target to make tumor cells prone to growth inhibition or apoptosis [8]. It has been shown that STAT3 protein is constitutively active in many tumor tissues, including those derived from BC patients [9, 10]. STAT3 protein can be involved in breast tumor formation through various pathways [11, 12]. This protein can be activated by the leukemia inhibitory factor (LIF) in normal breast cells, while it is triggered by IL-6 stimulation in BC [13]. Additionally, intrinsic kinases such as epidermal growth factor receptor (EGFR) and vascular endothelial growth factor receptor (VEGFR) can cause abnormal phosphorylation of STAT3 in BC [14]. Once activated, this transcription factor can regulate growth, survival, and metastasis in BC, as well as result in resistance to chemotherapy and radiotherapy. So, the therapeutic inhibition of STAT3 signaling may be efficient in BC [15].

Despite the safety of CUR at very high concentrations, its therapeutic potential is restricted due to low bioavailability. Insufficient absorption, rapid metabolism, and rapid systemic elimination might explain the reason for its poor systemic availability when administered orally. Nano-formulation of CUR is an efficient approach to improve its bioavailability and pharmacokinetics, which enhances its therapeutic advantages and betters its binding, internalization, and tumor-targeting properties. For this reason, various nanostructures designed to carry CUR, such as nano-capsules, have been studied and their anti-cancer effects have been investigated [16]. Nano-capsules have shown a significant decrease in IC50, indicating an increase in the anti-cancer activity of curcumin after encapsulation [17, 18]. Carbon-based nanomaterials have also been used as carriers of CUR [19], which have been shown relatively high toxicity against breast cancer cells [20]. Recently, selenium (Se) NPs have received a great deal of attention in the field of anticancer drug carriers. The role of Se in cancer prevention and reduction of drug toxicity make Se NPs superior to existing approaches including biogenetic and synthetic [21].

Targeted delivery is an important issue for cancer therapy and diagnosis. The high affinity of folic acid (FA) to folate receptors on the surface of various cancer cells makes this active targeting ligand as the first candidate for selective localization of therapeutic or diagnostic agents in cancer cells [22].

This prompted us to synthesis the CUR-loaded FA conjugated NPs and examine whether it could efficiently inhibit aberrantly activated STAT3 in breast cancer (MCF7) cells (Fig. 1).

Experimental

Materials

CUR, sodium selenite (Na_2SeO_3), and FA were obtained from Sigma (St. Louis, MO, USA). Ascorbic acid was purchased from Carl Roth GmbH + Co. KG. The primary antibodies (β-Actin (C4): sc-47778, p-Stat3 (B-7): sc-8059, and Stat3 (F-2): sc-8019) and secondary antibodies (mouse anti-rabbit IgG-HRP: sc-2357) were obtained from Santa Cruz Biotechnology, Inc. Fetal bovine serum (FBS), Penicillin–Streptomycin (PEN/STREP), trypsin, and RPMI medium were purchased from BioIdea, Iran.

Synthesis and Characterization of FA-Se@CUR NPs

FA-Se NPs were synthesized as previously reported by Shahverdi et al. [23] with some modifications. Briefly, a 2.6 mL FA solution (1 g/L) and 300 µL Na_2SeO_3 solution (50 mM) were mixed. A 2.4 mL aqueous ascorbic acid solution (50 mM) was added dropwise to the above mixture with magnetically stirring for 30 min at room temperature. Finally, the reaction mixture was centrifuged at 8000 rpm for 10 min and washed three times with double-distilled water to remove unreacted materials. Afterward, 4 mg of CUR was dissolved in 100 µl of dimethyl sulfoxide (DMSO) and then added into FA-Se NPs solutions under stirring for 30 min to make FA-Se@CUR NPs. The chemical structure of nanoparticles was characterized by Fourier-transform infrared spectroscopy (FTIR), Dynamic light scattering (DLS) analysis, and transmission electron microscope (TEM).

FTIR

The formation of covalent bonds between Se-NPs and CUR was assessed by FTIR spectroscopy. The FTIR sample spectrum was obtained by Potassium Bromide (KBr) disk technique on a single beam Perkin Elmer Spectrum II

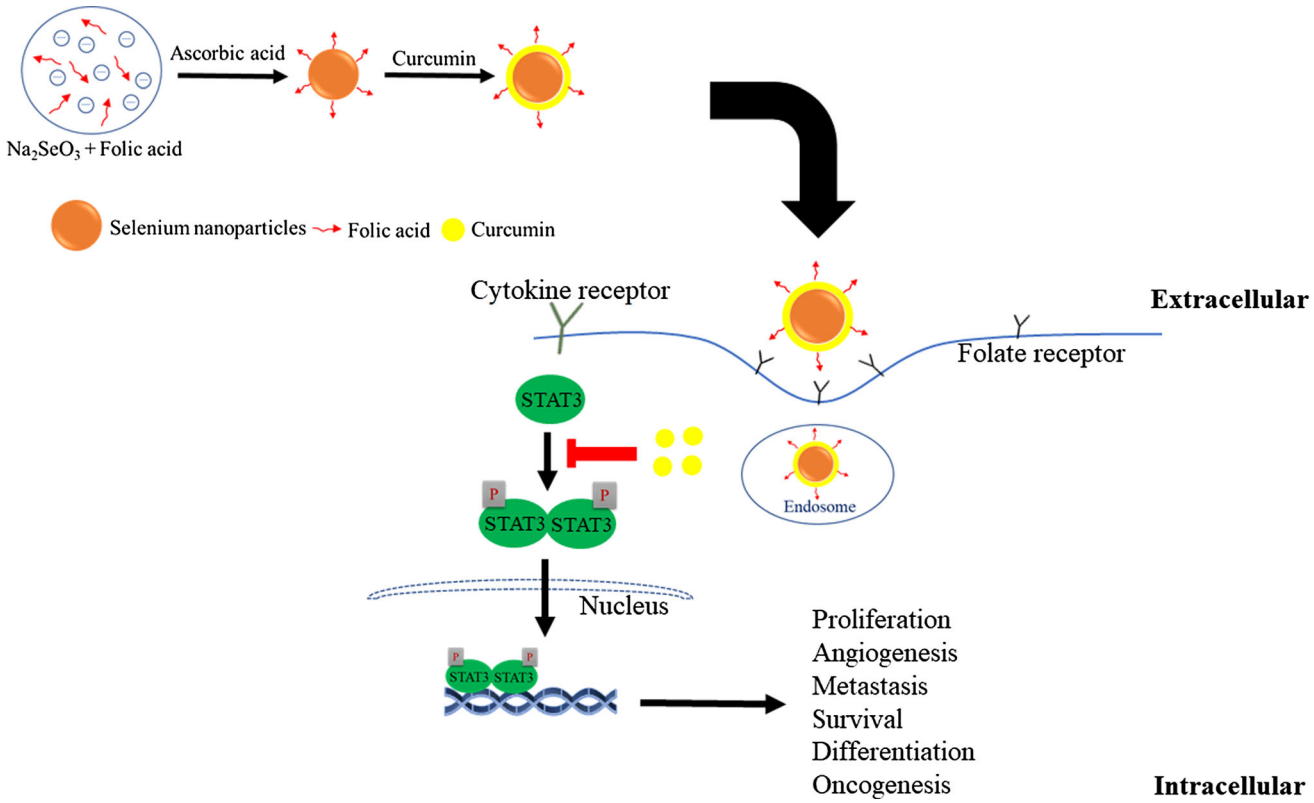

Fig. 1 Schematic illustration of the synthesis of FA-Se@CUR NPs and their mechanism of action

Spectrometer (Llantrisant, UK) over a range of 4000–400 cm^{-1}.

DLS

The average particle diameter and zeta potential of NPs were defined by DLS using NP size, zeta potential, and molecular weight analyzer SZ-100 HORIBA Scientific. Measurements were performed automatically in triplicates with a temperature of 25 °C and a dispersion medium viscosity of 0.89 mPa·s.

TEM

The size and morphology of NPs were determined by TEM. First, the NPs were dissolved in water at a concentration of 1 mg/ml by sonication. Next, a drop of the solution was placed over carbon-coated copper grids and air-dried at room temperature. The micrographs were obtained on a TEM (Leo 906 E TEM, Zeiss, Germany) operated at an accelerating voltage at 100 kV.

Cell Line and Cell Culture

The MCF-7 cancer cell line (ATCC® HTB-22TM) was purchased from the cell bank at the Pasteur Institute (Tehran, Iran). All the reagents and mediums were prepared immediately before application in the current work.

MCF-7 cells were cultured in RPMI medium supplemented with 10% FBS, PEN/STREP (1% v/v). Then, the cells were incubated at 37 °C in 5% CO2.

MTT Assay

The effects of CUR and NPs on the viability of the MCF-7 cells were evaluated using MTT assay. In brief, the cells were seeded onto a 96-well culture plate containing 100 µl of growth medium at a density of 5000 cells per well and then incubated for 24 h in 5% CO2 at 37 °C. Next, cells were exposed to CUR, Se-Cur, and FA-Se@CUR at different concentrations: 0 µM, 10 µM, 30 µM, 60 µM, 120 µM for 24 h at 37 °C in 5% CO2. The old medium was substituted with 20 µl of MTT solution (0.5 mg/mL). After a 3.5-hour incubation, the formazan precipitate was dissolved in 200 µl of DMSO. Lastly, the absorption of the solution was quantified by an ELISA reader (State Fax® 2100, Awareness, USA) at 570 nm. The percentage of cytotoxicity was calculated with the following equation:

$$\%Cytotoxicity = (100 \times (control - sample))/sample$$

The half-maximal inhibitory concentrations (IC50) were determined as µg/ml.

Preparation of Cell Lysates and Western Blot

After 24-h treatment with CUR, Se-Cur, and FA-Se@CUR, cells were collected and washed with cold PBS and resuspended in ice-cold EBC lysis buffer (500μL Tris–HCL, pH 8, 0.08gr NaCl, 0.003gr EDTA, 0.025gr Sodium Deoxycholate, 0.01gr SDS, and 10 μl NP-40/Triton X-100) containing protease inhibitor cocktail (1 tablet). After cell lysis and centrifugation at 12,000×g for 10 min at 4 °C, the resulting supernatant was gathered as the whole cell lysate. Proteins were quantified using the Bradford assay, then separated by sodium dodecyl sulfate-polyacrylamide gel electrophoresis (SDS-PAGE) and transferred to polyvinylidene difluoride (PVDF) membranes (EMD Millipore). PVDF membranes were incubated overnight with primary antibodies at 4 °C. The next day, after incubation with peroxidase-conjugated anti-rabbit IgG at 37 °C for 2 h, protein levels were visualized by electrochemiluminescence. Untreated MCF-7 whole cell lysate was considered as a control group.

Statistical Analysis

All the experiments were repeated three times independently and the data has been expressed as mean ± SD. Statistical analysis was done using SPSS software ver. 26.0 (IBM, Armonk, NY, USA) and one-way ANOVA test was used to compare a difference between the control and treatment groups. A p value of ≤ 0.05 is regarded as significant.

Results

Characterization of FA-Se@CUR Nanoparticles

FTIR absorbance spectrum was utilized to verify the successful modification of Se NPs with FA and CUR molecules (Fig. 2). The FT-IR spectrum of FA-Se@CUR NPs indicated a carbonyl band at 1630.44 cm^{-1} and a peak at 3434 cm^{-1} for phenolic hydroxyl groups.

The size and surface charge (zeta potential) of NPs can affect their cellular internalization. So, the size and zeta potential of NP were determined using DLS. The size of FA-Se@CUR NPs was found to be ∼ 130 nm (PI – 0.27). Also, the zeta potential of NPs was ∼ 45 mV (Fig. 3a). Figure 3b shows the average size of the NPs lacking CUR to compare with FA-Se@CUR NPs. In previous studies [23, 24], the average size of Se NPs and Se-FA NPs were about 60 and 100 nm, respectively.

The particle morphology by TEM (Fig. 4) for NPs were found to be spherical. Also, the FA-Se@ CUR NPs obtained were in the size range of 50–200 nm (Fig. 4).

The Results of the MTT Test

The MTT test indicated that increasing concentrations of drugs (CUR, Se-Cur, and FA-Se@CUR) gradually increase cytotoxicity. However, at a concentration of 60 μM, FA-Se@CUR reduced cell viability rate up to 49.62 ± 1.85% ($p < 0.05$), which was more than Se-Cur (36.19 ± 5.63%) and CUR (31.44 ± 8.96%). The IC50 value for FA-Se@CUR NPs was considered 60 μM (20 μg/ml), which inhibits cell growth by 50%. Figure 5 presents the cytotoxicity effect of drugs on cells after treatment for 24 h.

STAT3 Protein Analysis with Western Blot

To specify whether treatment of FA-Se@CUR NPs influences the expression of the STAT3 or its phosphorylation in MCF-7 cells, the expression of STAT3 and p-STAT3 was quantified by western blot analysis. In the present study, we found that the level of both p-STAT3 and STAT3 were reduced in FA-Se@CUR NPs exposed cells (Fig. 6a). At concentration of 60 μM FA-Se@CUR, the downregulation of total STAT3 was achieved to be 1.5-fold ($P < 0.0001$) while p-STAT3 indicated 4.8-fold ($P < 0.0001$) reduction (Fig. 6b). Also, compared with the control group, the quantity of STAT3 and p- STAT3 was decreased up to 1.26 and 2.17 or 1.25 and 2.63 after treatment with CUR and Se-CUR NPs, respectively.

Discussion

Breast cancer ranks fifth in cancer mortality globally and is also the most frequent cause of cancer death for women worldwide [25, 26]. The high cost and side effects of chemotherapy for treating breast cancer have made this disease one of the most controversial health problems. So, there is still a need to search for low-cost treatments with fewer adverse effects.

Persistent activation of STAT3 is found with high frequency in all breast cancer subtypes. The results obtained from modulating STAT3 constitutive activation using genetic and pharmacological methods in various experiments have provided convincing evidence for STAT3's important function in the development and progression of BC [27, 28]. STAT3 activation occurs following phosphorylation of tyrosine 705 (Tyr705) residue, which leads to dimerization and transport of STAT3 from the cytoplasm to the nucleus, where its binding to target genes stimulates the transcription [29]. STAT3 promotes

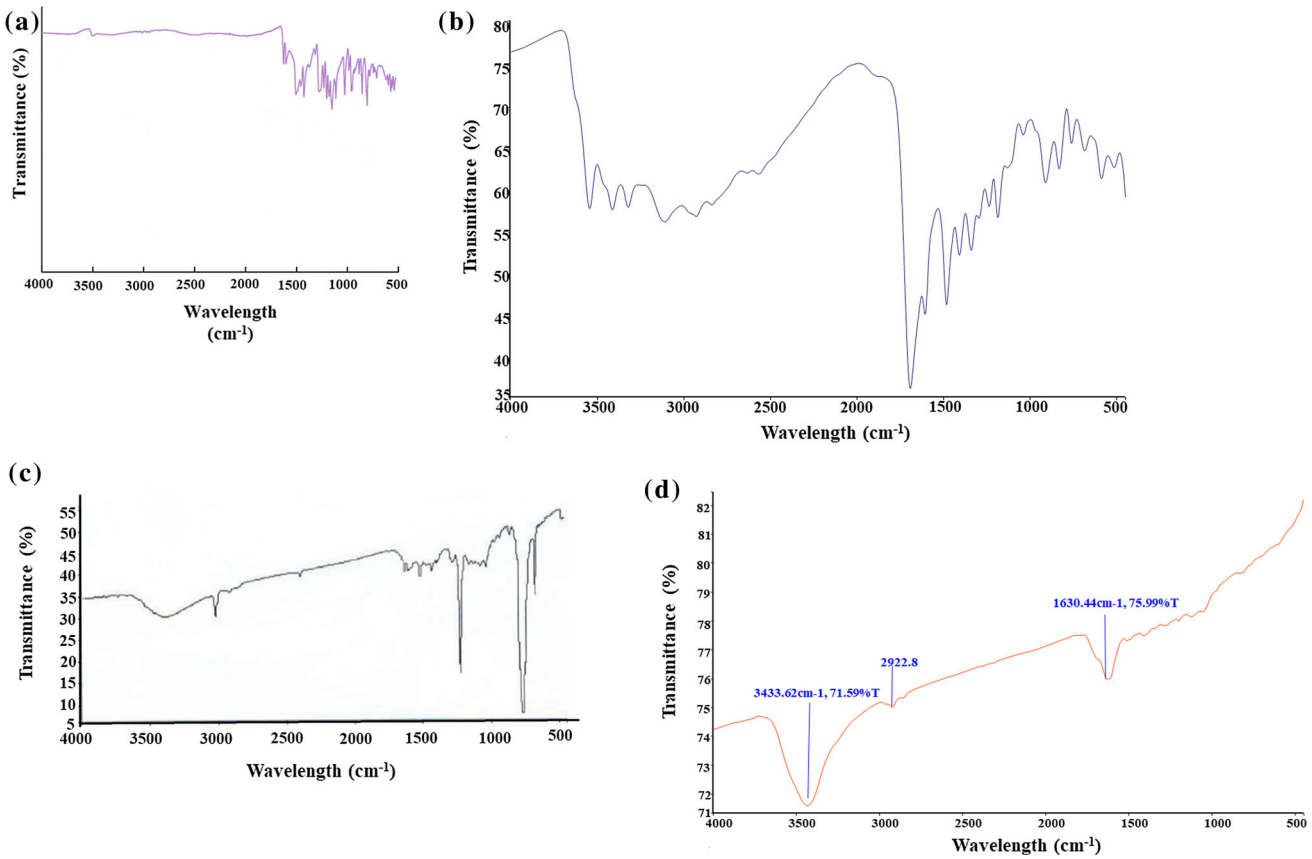

Fig. 2 FTIR absorbance spectrum of **a** CUR, **b** FA, **c** Se NPs, and **d** FA-Se@CUR NPs

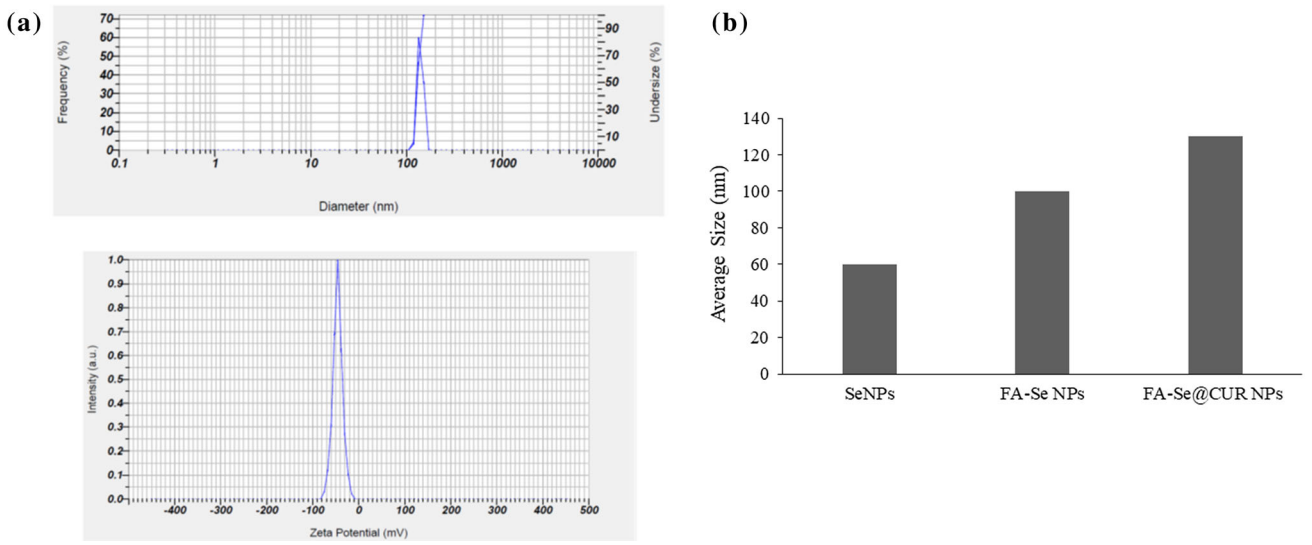

Fig. 3 **a** Particle size and zeta potential distribution of FA-Se@CUR NPs, and **b** comparison of the size of CUR-containing NPs with CUR-free NPs

malignancy by deregulating main proteins that control proliferation (Bcl-xL, Bcl-2, Mcl-1, survivin, cyclin D1/D2, and c-Myc), angiogenesis (VEGF), and epithelial-mesenchymal transition (MMP-2, MMP-9) [30, 31]. The vital role of STAT3 in cancer progression and tumorigenesis makes it a promising molecular target for cancer treatment. So, it is necessary to find a strong small molecule that can significantly inhibit STAT3 activation.

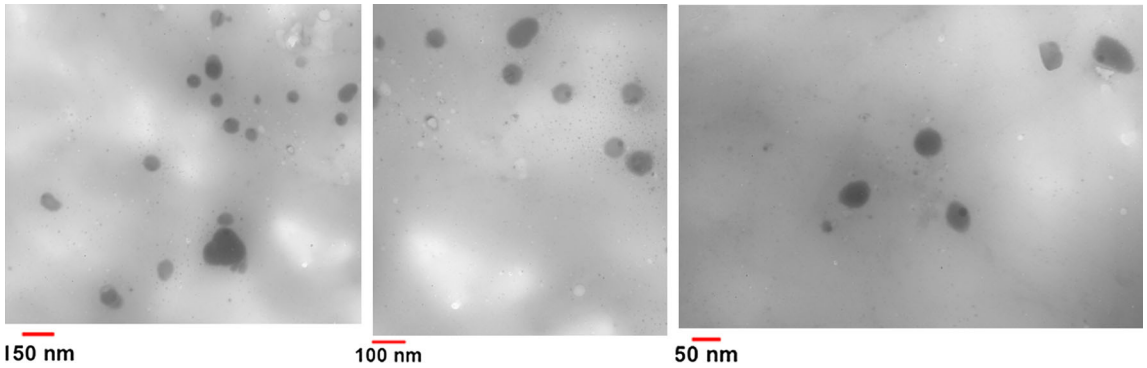

Fig. 4 TEM images from FA-Se@CUR NPs in different sizes

Fig. 5 The cytotoxicity effect of different concentrations of CUR and NPs on breast cancer cells (MCF7) after treatment for 24 h. Statistically different results compared to untreated cells are indicated with *($p < 0.05$)

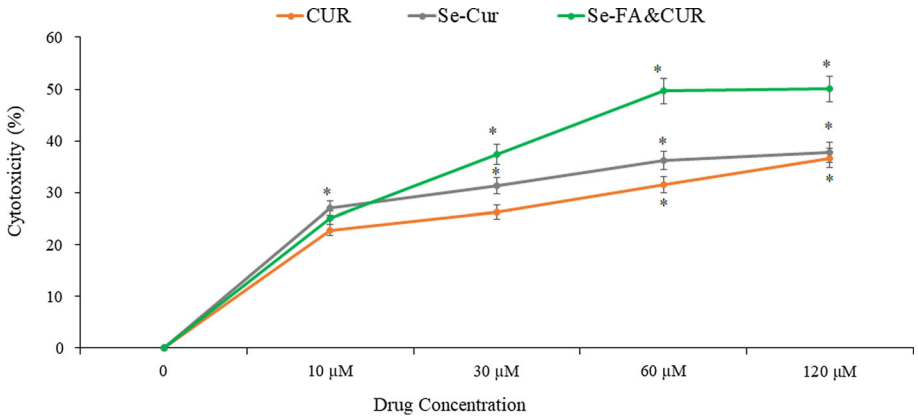

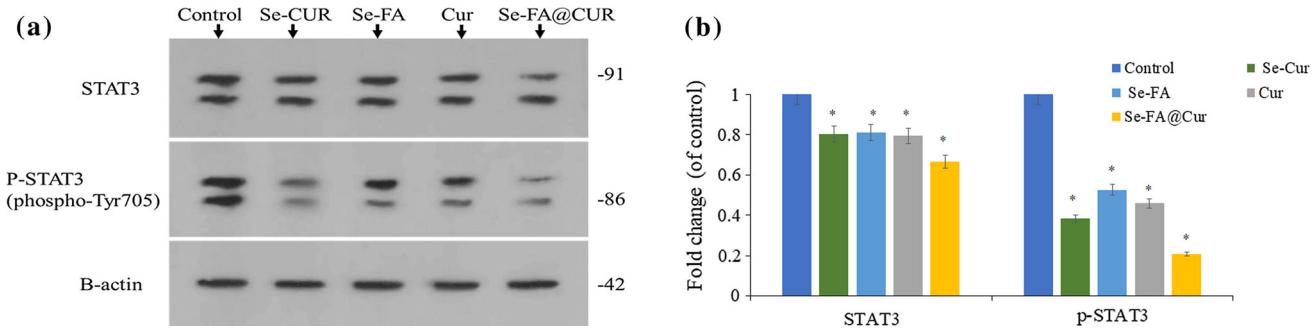

Fig. 6 **a** Western blot image of STAT3 and p-STAT3 in different treated groups, and **b** Representative bar diagram indicating fold change of STAT3 and p-STAT3 to the control in different treated groups (*$p < 0.0001$ Control versus treated groups)

Although various studies have shown that CUR is a safe and effective inhibitor of STAT3 in several tumors [32, 33], its poor bioavailability inhibits its chemotherapeutic application [34]. Nanotechnology has been employed to solve this problem. For this reason, we introduced the FA-Se@CUR NPs as a cancer-targeting delivery system to attain enhanced anticancer efficacy. The present study hypothesized that the surface binding of curcumin over FA-Se NPs may provide stable NPs with a high-surface negative-charge. Furthermore, the stable, nano-sized, colloidal particles may cause the solubility of curcumin in the aqueous media, as opposed to CUR, which is virtually insoluble in aqueous media. Moreover, the results of previous studies have demonstrated that FA surface modification significantly increases the cellular uptake of NPs in folate receptor over-expressed cancer cells including MCF-7 cells [35, 36]. Overexpression of folate receptors on the surface of various tumor types can be used to target therapeutic compounds directly to cancerous tissues in many ways. Therefore, in this study, folate was loaded on the surface of the NPs to facilitate the active transport of NPs to the cell. The synthesis of FA-Se@CUR NPs was performed by reducing Na_2SeO_3 to Se^0 by ascorbic acid, and curcumin was attached to Se^0 by

forming the Se-O co-ordinate bonds and physical adsorption. According to the DLS results, the average size of the prepared NPs was 130 nm, and their small size may enhance their therapeutic ability mainly due to better passive targeting. They were also monodispersed and displayed a high absolute zeta potential value of -45 mV (Fig. 3 & 4). The Negative value of the zeta potential of the NPs is probably due to the ionized carboxylic groups of FA. Also, the large amount of surface charge may prevent the accumulation of NPs by generating electrostatic repulsion, which increases the colloidal stability of NPs. According to a study by Duffy et al., the suspensions with an absolute zeta potential value of more than 30 mV are considered stable [37].

Furthermore, in the present study, the effects of nano-formulated CUR on MCF7 cell line viability were investigated. According to the results, at a concentration of 60 μM, FA-Se@CUR NPs reduced cell viability rate up to 49.62 ± 1.85%, which was more than by Se-Cur (36.19 ± 5.63%) and CUR (31.44 ± 8.96%). This demonstrates that FA-Se@CUR has more potential to induce cytotoxicity in MCF7 cell line than curcumin and Se-Cur NPs. Also, the more reduction in survival in cells exposed to FA-Se@CUR than in cells exposed to Se-Cur may be due to greater uptake of folate conjugated NPs into cells via the folate receptor. According to previous studies, MCF-7 cells present the constitutive activation of STAT3. So, MCF-7 cells were treated with FA-Se@CUR, Se-CUR, Se-FA, and CUR at a concentration of 60 μM for 24 h, and the level of STAT3 and the activated form of STAT3 (pSTAT3) were checked by immunoblotting. Cells treated with FA-Se@CUR showed a stronger decline in levels of STAT3 (up to 33.5%) and p-STAT3 (up to 79%) than control (untreated) as well as other treated groups. In the group treated with Se-CUR, the amount of STAT3 decreased by 20% and p-STAT3 by 62% compared to the control. Interestingly, the results obtained are in accordance with those of the MTT test. These findings suggest that STAT3 phosphorylation is more effectively inhibited by nano-formulated CUR, which is comparable to results previously proven for CUR [38]. A study by Song Y et al. showed that constant expression of active STAT3 increases matrix metalloproteinase-9 (MMP-9) mRNA levels in MCF-7 cells, suggesting that it is also regulated by STAT3 [39]. Also, while testing the effect of hydrazine-curcumin (HC), a synthetic curcumin analog, suppression of STAT3 phosphorylation in breast cancer cell lines (MDA-MB-231, MCF-7) reduced the expression of c-Myc, Bcl-xL, Bcl-2, Mcl-1, cyclin D1/D2, VEGF, MMP-2, and MMP-9 [34].

Therefore, this drug may alter the expression of some important genes in carcinogenesis by significantly reducing the amount of phosphorylated STAT3, which has not been evaluated in this study due to financial constraints.

Conclusion

The ability to inhibit STAT3 phosphorylation suggests that FA-Se@CUR could be an alternative or additional option in the treatment of breast cancer.

Acknowledgments The study was supported and funded by the Deputy of Research and Technology, Ardabil University of Medical Sciences, IR.ARUMS.REC.1398.340.

Author contributions EF carried out most of the experiments leading to the synthesis of nanoparticles, contributed to the design and the supervision of the study, analyzed the data, prepared the figures, and wrote the manuscript. The author has no conflict of interest. MS supervised the study and corrected the manuscript. The author has no conflict of interest. AHF modified the text and corrected the manuscript. The author has no conflict of interest.

Declarations

Conflict of interest The authors report no conflicts of interest.

References

1. C. M. Rodríguez-Razón, I. Yañez-Sánchez, V. O. Ramos-Santillan, and C. Velásquez-Ordóñez (2018). *Int. J. Nanomed.* **13**, 1081–1095.
2. J. Ferlay, I. Soerjomataram, R. Dikshit, S. Eser, C. Mathers, M. Rebelo, et al. (2015). *Int. J. Cancer* **136**, E359.
3. C. Pan, Y. Liu, M. Zhou, W. Wang, M. Shi, M. Xing, et al. (2018). *Int. J. Nanomed.* **13**, 1119.
4. S. A. Mousa and D. J. Bharali (2011). *Cancers (Basel).* **3**, 2888.
5. S. Banerjee Nanoparticle-Based Delivery of Phytochemical Compounds Against Major Maladies: Cancer, Diabetes, and Cardiovascular Disease. in M. Swamy (ed.), *Plant-derived Bioactives* (Springer, Singapore, 2020).
6. M. M. Yallapu, M. Jaggi, and S. C. Chauhan (2013). *Curr. Pharm. Des.* **19**, 1994.
7. M. M. Yallapu, M. Jaggi, and S. C. Chauhan (2012). *Drug Discov. Today.* **17**, 71.
8. Y. I. Hahn, S. J. Kim, B. Y. Choi, K. C. Cho, R. Bandu, K. P. Kim, et al. (2018). *Sci Rep.* **8**, 6409.
9. M. Lee, J. L. Hirpara, J.-Q. Eu, G. Sethi, L. Wang, B.-C. Goh, et al. (2019). *Redox Biol.* **25**, 101073.
10. A. L. A. Wong, J. L. Hirpara, S. Pervaiz, J. Q. Eu, G. Sethi, and B. C. Goh (2017). *Expert Opin. Investig. Drugs* **26**, 883.
11. K. Hughes and C. J. Watson (2018). *Int. J. Mol. Sci.* **19**, (6), 1694.
12. F. Laudisi, F. Cherubini, G. Monteleone, and C. Stolfi (2018). *Int J Mol Sci.* **19**, 1787.
13. T. Ara and Y. A. Declerck (2010). *Eur. J. Cancer* **46**, 1223.
14. B. S. Yadav, P. Chanana, and S. Jhamb (2015). *World J Clin Oncol.* **6**, 252.
15. L. L. Marotta, V. Almendro, A. Marusyk, M. Shipitsin, J. Schemme, S. R. Walker, et al. (2011). *J Clin Invest.* **121**, 2723.
16. E. Gholibegloo, T. Mortezazadeh, F. Salehian, A. Ramazani, M. Amanlou, and M. Khoobi (2019). *Carbohydr. Polym.* **213**, 70.
17. L. Bechnak, C. Khalil, R. El Kurdi, R. S. Khnayzer, and D. Patra (2020). *Photochem. Photobiol. Sci.* **19**, 1088.
18. L. Slika, A. Moubarak, J. Borjac, E. Baydoun, and D. Patra (2020). *Mater. Sci. Eng. C* **109**, 110550.
19. B. Barzegarzadeh, H. Hatami, G. Dehghan, N. Khajehnasiri, M. Khoobi, and R. Sadeghian (2021). *Neurotoxicity Res.* **39**, 815.

20. M. Razaghi, A. Ramazani, M. Khoobi, T. Mortezazadeh, E. A. Aksoy, and T. T. Küçükkılınç (2020). *J. Drug Deliv. Sci. Technol.* **60**, 101967.
21. J. Zou, S. Su, Z. Chen, F. Liang, Y. Zeng, W. Cen, et al. (2019). *Artif. Cells Nanomed. Biotechnol.* **47**, 3456.
22. E. Gholibegloo, T. Mortezazadeh, F. Salehian, H. Forootanfar, L. Firoozpour, A. Foroumadi, et al. (2019). *J. Colloid Interface Sci.* **556**, 128.
23. A. R. Shahverdi, F. Shahverdi, E. Faghfuri, F. Mavandadnejad, M. H. Yazdi, and M. Amini (2018). *Arch. Med. Res.* **49**, 10.
24. E. Faghfuri, M. H. Yazdi, M. Mahdavi, Z. Sepehrizadeh, M. A. Faramarzi, F. Mavandadnejad, et al. (2015). *Arch. Med. Res.* **46**, 31.
25. C. Fitzmaurice, C. Allen, R. M. Barber, L. Barregard, Z. A. Bhutta, H. Brenner, et al. (2017). *JAMA Oncol.* **3**, 524.
26. N. Azamjah, Y. Soltan-Zadeh, and F. Zayeri (2019). *Asian Pac. J. Cancer Prev. APJCP.* **20**, 2015.
27. P. Yue and J. Turkson (2009). *Expert Opin. Investig. Drugs* **18**, 45.
28. H. Yu and R. Jove (2004). *Nat. Rev. Cancer* **4**, 97.
29. J. Bromberg and J. E. Darnell Jr. (2000). *Oncogene* **19**, 2468.
30. J. Turkson (2004). *Expert Opin Ther Targets.* **8**, 409.
31. K. Banerjee and H. Resat (2016). *Int. J. Cancer* **138**, 2570.
32. A. Pandey, K. Vishnoi, S. Mahata, S. C. Tripathi, S. P. Misra, V. Misra, et al. (2015). *Nutr. Cancer* **67**, 1293.
33. A. R. Fetoni, F. Paciello, D. Mezzogori, R. Rolesi, S. L. Eramo, G. Paludetti, et al. (2015). *Br. J. Cancer* **113**, 1434.
34. X. Wang, Y. Zhang, X. Zhang, W. Tian, W. Feng, and T. Chen (2012). *Int. J. Oncol.* **40**, 1189.
35. G. L. Zwicke, G. A. Mansoori, and C. J. Jeffery (2012). *Nano Rev.*. https://doi.org/10.3402/nano.v3i0.18496.
36. J. Pi, H. Jin, R. Liu, B. Song, Q. Wu, L. Liu, et al. (2013). *Appl. Microbiol. Biotechnol.* **97**, 1051.
37. J. Duffy, M. Larsson, and A. Hill (2012). *Annu. Trans. Nordic Rheol. Soc.* **20**, 6.
38. W. Glienke, L. Maute, J. Wicht, and L. Bergmann (2010). *Cancer Invest.* **28**, 166.
39. Y. Song, L. Qian, S. Song, L. Chen, Y. Zhang, G. Yuan, et al. (2008). *Mol. Immunol.* **45**, 137.